A Pre-Clinical Animal Study for Zonal Articular Cartilage Regeneration Using Stratified Implantation of Microcarrier Expanded Zonal Chondrocytes

Ching Ann Tee[1,2] (iD), Zheng Yang[1,3], Yingnan Wu[1,3], Xiafei Ren[1,3], Maciej Baranski[2], Daryl Jimian Lin[1,3], Afizah Hassan[1,3], Jongyoon Han[2,4], and Eng Hin Lee[1,2,3]

Abstract

Objective. The zonal properties of articular cartilage critically contribute to the mechanical support and lubrication of the tissue. Current treatments for articular cartilage have yet to regenerate this zonal architecture, thus compromising the functional efficacy of the repaired tissue and leading to tissue degeneration in the long term. In this study, the efficacy of zonal cartilage regeneration through bilayered implantation of expanded autologous zonal chondrocytes was investigated in a porcine chondral defect model. *Design.* Autologous chondrocytes extracted from articular cartilage in the non-weight bearing trochlea region of the knee were subjected to an expansion-sorting strategy, integrating dynamic microcarrier (dMC) culture, and spiral microchannel size-based zonal chondrocyte separation. Zonal chondrocytes were then implanted as bilayered fibrin hydrogel construct in a porcine knee chondral defect model. Repair efficacy was compared with implantation with cell-free fibrin hydrogel and full thickness (FT) cartilage-derived heterogenous chondrocytes. Cartilage repair was evaluated 6 months after implantation. *Results.* Sufficient numbers of zonal chondrocytes for implantation were generated from the non-weight bearing cartilage. Six-month repair outcomes showed that bilayered implantation of dMC-expanded zonal chondrocytes resulted in substantial recapitulation of zonal architecture, including chondrocyte arrangement, specific Proteoglycan 4 distribution, and collagen alignment, that was accompanied by healthier underlying subchondral bone. *Conclusion.* These results demonstrate that with appropriate expansion and isolation of zonal chondrocytes, the strategy of stratified zonal chondrocyte implantation represents a significant advancement to Autologous Chondrocyte Implantation-based cartilage regeneration, with the potential to improve the long-term integrity of the regenerated tissues.

Keywords

articular cartilage, zonal chondrocytes, inertial spiral microchannel, dynamic microcarrier culture, autologous chondrocyte implantation

Introduction

The zonal organization of articular cartilage is critical for the biphasic mechanical properties of the tissue to provide lubrication and load transmission during the joint motion. Articular cartilage can be separated into superficial zone (SZ), middle zone (MZ), and deep zone (DZ).[1,2] Across the zones, they are different in terms of chondrocyte morphology and size, collagen organization, and extracellular matrix composition. In SZ, the chondrocyte is relatively small and has an elongated morphology. The collagen in the SZ is tightly packed and aligned parallel to the articulating surface, providing high tensile strength at the articular surface,[3] and act as a permeability barrier facilitating generation

of fluid load support in the underlying zones.[4,5] Proteoglycan 4 (PRG4), secreted specifically by SZ chondrocytes, acts as lubricant to provide frictionless joint motion.[6] Going deeper into the articular cartilage, the chondrocytes increase in size and have rounded morphology. MZ has randomly organized collagen fibrils, while the collagen alignment in DZ is perpendicular to the articulating surface and this alignment was shown to be important in resisting the compressive force in the deeper zone.[7,8] The collagen fibrils in deep zone are anchored to the subchondral bone, securing the cartilage to the underlying bone to maintain the structural integrity of osteochondral unit.[3,9] The high concentration of Type II Collagen (Col2) and Aggrecan (Agg) in the MZ and DZ endows the tissue with a high osmotic pressure to withstand

the compressive force. Minor proteins such as cartilage oligomeric matrix protein (COMP) and Type IX Collagen (Col9) are also present specifically in the deeper zones to regulate the collagen fiber size, inter-fiber cross linking and interaction with Agg.[10,11]

The avascular nature of articular cartilage has limited its self-healing capability. Autologous Chondrocyte Implantation (ACI) is the only cell-based therapy currently approved by FDA for treatment of injury-induced articular cartilage lesions. Although the short-term outcomes of ACI treatment showed improved tissue regeneration, the integrity of the regenerated tissues degenerated in the long-term.[12] One of the possible reasons could be the implantation of a heterogeneous mixture of chondrocytes which may not have the ability to reproduce the zonal architecture of normal cartilage. Zonal chondrocyte subpopulations were shown to crosstalk and influence each other's phenotypes. The presence of SZ chondrocytes increased the proliferative and biosynthetic activities of DZ chondrocytes.[13-15] On the other hand, the presence of DZ chondrocytes decreased the GAG secretion of SZ,[15] while upregulating the secretion of PRG4 in SZ chondrocytes.[13] Recapitulation of zonal architecture in regenerated tissues has thus been hypothesized to improve the quality of regenerated cartilage.[16,17]

Various efforts have been attempted to recreate the zonal architecture of articular cartilage employing heterogenous chondrocytes with the use of multi-layered composite scaffold that mimic the structural design, chemical cues, and mechanical characteristics of mature articular cartilage to guide the morphology, orientation, and phenotypic state of chondrocytes. Polymer scaffolds fabricated with pore-size gradients was shown to promote the anisotropic cell distribution and matrix contents similar to that in superficial, middle, and deep zones of articular cartilage.[18] Hybrid hydrogel scaffold with electrospun nanofiber mesh of different orientation was employed to stimulate cellular morphology and ECM contents assembling zonal cartilage.[19] A multi-zonal nanocomposite scaffolds that mimics the distinct collagen orientation and matric components of zonal cartilage support the growth of tissue that are reminiscent of the natural analogue.[20] 3D bio-printed scaffold with different cell densities mimicking cell gradient of the human articular cartilage zones were also studied.[21] On the other hand, formation of stratified tissue constructs with zonal chondrocytes require a relatively simpler scaffold design due to their intrinsic zonal phenotypes.[16,17] Zonal chondrocytes were utilized to form multi-layered cartilage constructs via layer by layer seeding of zonal chondrocytes at high density on the hanging well.[22] The multilayer architecture of the constructs was able to be maintained after 4 weeks of culture *in vitro*.[23,24] Multilayer agarose hydrogel of different concentrations[14,25] and photo-crosslinkable hydrogel such as poly(ethylene oxide) diacrylate (PEODA)[15,26] containing zonal chondrocytes were also investigated to create multi-layered cartilage constructs. The tissue constructs formed depth-dependent ECM content and mechanical strength,[14,25] as well as a stronger mechanical property than single layered hydrogel contained only DZ chondrocytes.[15] However, the lack of an efficient zonal chondrocyte isolation protocol has hindered the clinical implementation of stratified zonal chondrocyte implantation.[16] Current methods of zonal tissue segregation are manual, labor-intensive, and lack specificity. Furthermore, the limited number of autologous chondrocytes available from patients has entailed prolonged chondrocyte expansion that has led to zonal phenotype and functional loss.[27] A more efficient zonal chondrocyte isolation method, couples with a chondrocyte expansion protocol that maintain the zonal phenotype of the expanded cells is thus critical to realize the regeneration of articular cartilage zonal architecture through stratified implantation of zonal chondrocytes.

Toward this end, an inertial spiral microchannel device that performed high throughput label-free size-based cell separation was demonstrated to segregate and enrich zonal chondrocytes, derived from full thickness (FT) weight bearing (WB) articular cartilage tissue.[17] Delivery of the unexpanded zonal chondrocytes as bilayered fibrin hydrogel constructs in a proof-of-concept rat osteochondral defect study resulted in superior cartilage regeneration with mechanically enhanced tissues, in comparison to the implantation of FT cartilage-derived heterogenous chondrocytes.[17] A post-expansion cell sorting protocol was further developed that coupled dynamic microcarrier (dMC) expansion of FT chondrocytes followed by spiral microchannel sorting

[1]Department of Orthopaedic Surgery, National University of Singapore, Singapore
[2]Critical Analytics for Manufacturing Personalised-Medicine, Interdisciplinary Research Group, Singapore-MIT Alliance for Research and Technology, Singapore
[3]NUS Tissue Engineering Program, Life Science Institute, National University of Singapore, Singapore
[4]Department of Electrical Engineering and Computer Science, Department of Biological Engineering, Massachusetts Institute of Technology, Cambridge, MA, USA

Corresponding Author:
Eng Hin Lee, Department of Orthopaedic Surgery, National University of Singapore, 1E Kent Ridge Road, NUHS Tower Block 11, 119288 Singapore.
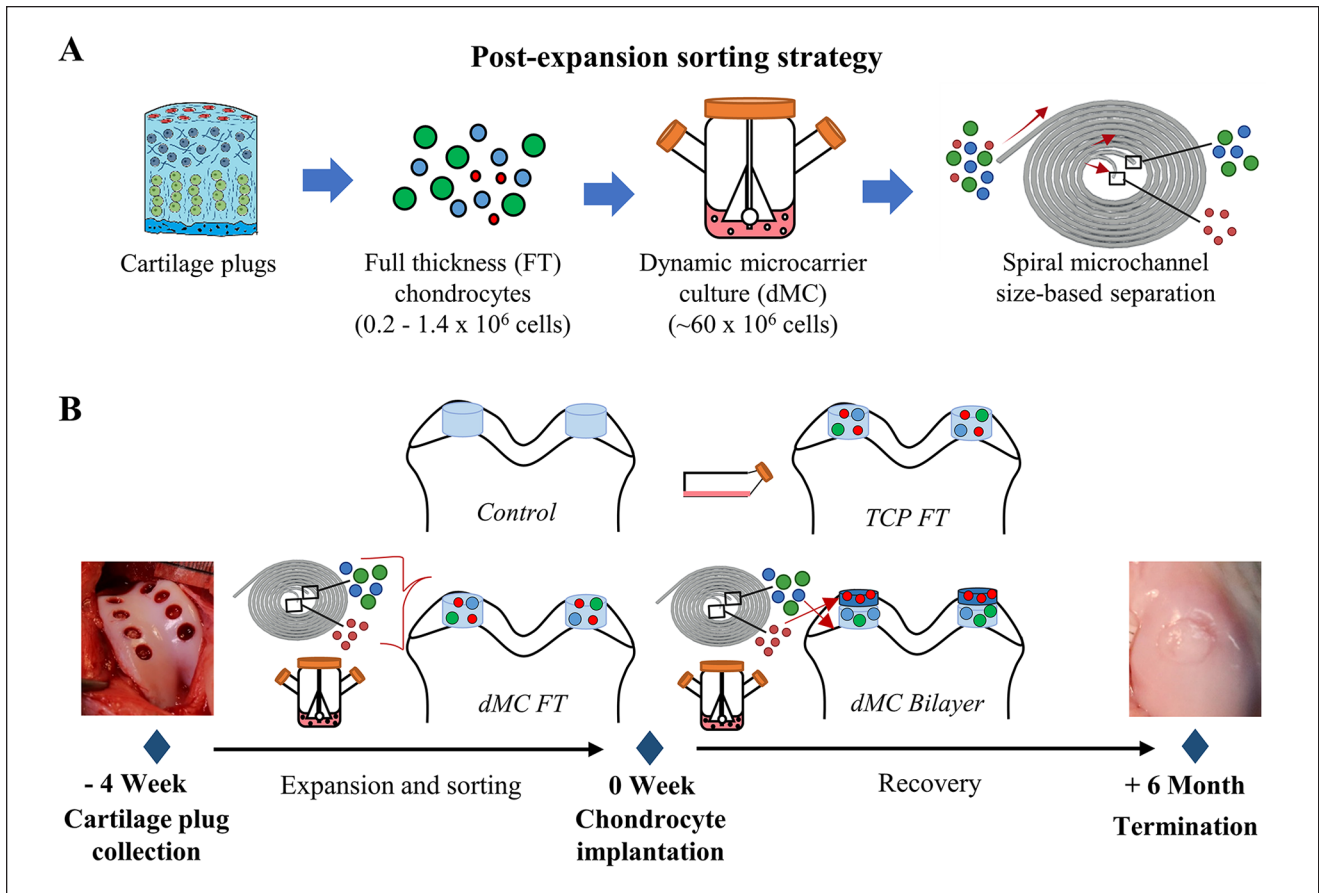Email: eng_hin_lee@nuhs.edu.sg

Figure 1. (**A**) Illustration of post-expansion sorting strategy. Full thickness (FT) chondrocytes were isolated from cartilage plugs. Cell number ranges from 0.2-1.4 x 10^6 of chondrocytes can be isolated from 0.5 cm^2 of articular cartilage. At the end of 4 weeks expansion, dynamic microcarrier culture yielded around 60 x 10^6 chondrocytes. Expanded chondrocytes were then subjected to size-based sorting using inertial spiral microchannel device to enrich zonal chondrocyte subpopulations. (**B**) Illustration of the animal surgery timeline. Non-weight-bearing articular cartilage plugs were collected 4 weeks before implantation for chondrocytes isolation, expansion, and size-based sorting to derived zonal chondrocytes. Animals were separated into 4 groups. Six months post-implantation, the femoral condyles with defects were collected for analysis. TCP = tissue plate culture platform.

(**Fig. 1A**).[28] In contrast to the observation that chondrocytes de-differentiated on static tissue plate culture platform (TCP), dMC culture not only preserved the zonal phenotype characteristics of the expanded chondrocytes, it also retained the zonal cell size and phenotype relation, hence enabling the performance of size-based separation on expanded FT chondrocytes. The dMC post-expansion sorting strategy thus made possible the generation of large quantities of zonal chondrocytes from the initially limited number of tissue-derived chondrocytes. Given that the autologous chondrocytes in the standard ACI protocol are derived from non-weight-bearing (NWB) cartilage plugs,[29] the purpose of this study was (1) to establish the applicability of dMC post-expansion sorting protocol[28] in yielding good quality zonal chondrocytes from NWB FT chondrocytes, in comparison with WB chondrocytes, and (2) to investigate the efficacy of bilayered implantation of the dMC-expanded autologous

zonal chondrocytes in cartilage zonal architecture regeneration using a porcine knee chondral defect model.

Methods

Primary Chondrocyte Isolation and Culture

WB and NWB chondrocytes were isolated from the femoral condyle and trochlea of articular cartilage, respectively, of 11 to 13 months old micropigs (PWG Genetics Pte Ltd, Singapore). Diced cartilage was digested in 0.25% (w/v) type-II collagenase overnight at 37°C. Isolated chondrocytes were sorted using the inertial spiral microchannel device, or expanded on tissue culture plate (TCP) for 1 passage. FT chondrocytes were seeded with an initial cell density of 5000 cells/cm^2 in a complete media containing low glucose Dulbecco's modified Eagle Medium (DMEM)

supplemented with 10% (v/v) fetal bovine serum (FBS), 1% GlutaMAX and 1% (v/v) penicillin-streptomycin at 37°C in 5% CO_2 atmosphere. All the reagents mentioned were purchased from Thermo Fisher Scientific.

Dynamic Microcarrier Culture

Cytodex® 1 microcarriers (Sigma-Aldrich) were prepared according to the manufacturer's protocol. Microcarriers were added to Corning® ProCulture® 125 ml glass spinner flask (Sigma-Aldrich) at a density of 10,000 microcarriers/ml in a total volume of 50 ml. TCP-passage 1 chondrocytes were seeded on microcarriers at an initial cell seeding density of 5000 cells/cm². In the first 6 hours, microcarriers and chondrocytes were cultured under intermittent stirring at 25 rpm for 2 minutes for every 30 minutes. The culture was kept static in the next 18 hours before continuous stirring regime at 60 rpm. The dynamic microcarrier culture was maintained for 2 passages at 8 days each. Chondrocytes were harvested with 0.1% (w/v) pronase solution (Sigma-Aldrich) and separated from microcarriers by passing through a 100 µm strainer (BD Bioscience, USA). Cell preparation was observed under microscope to ensure all the microcarriers were removed.

Chondrocyte Sorting With Inertial Spiral Microchannel Device

The schematic diagram of microchannel device and the illustration of the zonal chondrocyte distribution in the microchannel is shown in **Supplementary Figure S1**. The inertial spiral microchannel device was mounted on an inverted microscope (IX71, Olympus, Japan) equipped with a high-speed CCD camera (Phantom v9, Vision Research, USA) to visualize the separation of chondrocytes at real time as described elsewhere.[17,28] Large/DZ chondrocytes (S3) were first collected at the inner outlet after sorting at a higher flow rate. Cell suspension from the outer outlet was collected and pumped through the device again at a lower flow rate to separate and collect the medium size/MZ (S2) and small/SZ chondrocytes (S1) at inner and outer outlet respectively. The smallest 20% of the chondrocytes were collected as S1, 40% medium-sized chondrocytes as S2 and the largest 40% chondrocytes as S3.

Chondrocyte Re-Differentiation in Fibrin Hydrogel

Chondrocytes were suspended in 50 mg/ml fibrin provided in Fibrin Sealant Tisseel Kit (Baxter International Inc., USA). An equal volume of 10 IU thrombin solution was added to initiate gelation. The final cell density was 10 million cells/ml. The cell-hydrogel constructs were cultured for 3 weeks in the chondrogenic medium made of high glucose DMEM supplemented with 10^{-7} M dexamethasone, 1% ITS+ premix, 50 µg/ml ascorbic acid, 1 mM sodium pyruvate, 0.4 mM proline and 10 ng/ml of TGF-β3 (R&D System, USA).

Real-Time Polymerase Chain Reaction (qPCR) Analysis

Total RNA was extracted with the RNeasy® Mini Kit (Qiagen, Germany) and reverse transcription was performed using iScript™ cDNA synthesis kit (Bio-Rad, USA). Real-time PCR was carried out using POWER SYBR® green PCR master mix on ABI 7500 Real-time PCR System (Applied Biosystem, USA) at 95°C for 10 minutes and 40 cycles of amplification composed of 10 minutes of denaturation at 95°C and 1 minute extension at 60°C. The gene expression level was normalized to the commonly used reference gene, glyceraldehyde-3-phosphate dehydrogenase (*GAPDH*)[30,31] and was calculated using the formula, $2^{-\Delta\Delta Ct}$, with reference to undifferentiated porcine mesenchymal stem cells.

Histological and Immunohistochemical Staining

Hydrogel constructs were fixed in 10% neutral buffered formalin (Sigma-Aldrich) overnight at 4°C followed by graded ethanol dehydration and paraffin embedding. Cartilage tissues were decalcified before graded ethanol dehydration. Decalcification was performed at room temperature in 30% formic acid for 4 weeks with weekly change of decalcification solution. Samples were cut into 5 µm section using microtome (Leica, USA). Proteoglycan was stained with 0.1% Safranin O Solution (Acros Organics, USA) and counterstained with 0.02% Fast green solution (Sigma-Aldrich) and Accustain® Harris hematoxylin (Sigma-Aldrich). Immunohistochemical staining was performed to identify Col2, Type I Collagen (Col1), PRG4 and Col9 using Type II collagen mouse monoclonal antibodies (Clone 6B3 at 1:500 dilution, Chemicon, USA), Type I Collagen mouse monoclonal antibodies (1:500 dilution, Sigma-Aldrich), Lubricin rabbit polyclonal antibodies (ab-94933 at 1:100 dilution, Abcam, UK) and Type IX Collagen mouse antibodies (D1-9, B3-1 at 1:1000 dilution, Chondrex Inc., US). For Col2, Col1 and Col9 immunohistochemical staining, tissue sections were subjected to pepsin digestion for antigen retrieval. For PRG4 immunohistochemical staining, heat antigen retrieval was performed in sodium citrate buffer (10 mM sodium citrate, 0.05% Tween 20, pH 6.0). The Col9 and PRG4-positive cell were quantified manually from 3 hydrogel samples per group and 3 areas in each sample. The data were presented as the percentage of the positively stained cell.

Polarized Light Microscopy

Cartilage tissue sections were digested with 1 μg/ml of pepsin at 37°C for 30 mins and 4°C for the next 12 hours. The sections were then dehydrated and mounted. Visualization of collagen fiber orientation was carried out with Phoenix 5.0 MP Polarization camera (Lucid Vision Labs Inc., Canada) using circular polarization and filtered red light as input light.

Compression Test

Compression test was carried out using Instron tester 5567 (Singapore) at a compression rate of 0.01 mm/s with a 5 mm indenter to 50% strain for hydrogel constructs, or a 1 mm indenter to 30% strain for cartilage tissues. The compression tests were performed at 3 different locations on the cartilage defects. The strain was calculated using the formula, e = 1—L/L0 where L0 and L was the thickness of the hydrogel constructs before and after compression. The thickness of the cartilage before compression was 1 mm. Youngs' modulus was calculated using the formula, E = r/e, where r and e represent the stress and strain of the samples, respectively, derived from the stress-strain curve generated from the Bluehill software.

Tribology Test

The frictional properties of hydrogel constructs and cartilage tissues were measured using a nanotribometer (Anton Paar) with a sphere cantilever (spring constant: 7.5 N/m) and a 5 mm spherical borosilicate glass tips (Nova Scan). The measurement was performed with 20 cycles of linear movement at 3 different locations. The cantilever contact load was 0.2 mN and the sequence was performed at maximum linear speed of 0.15 mm/s with 1 mN normal load. The coefficient of friction was provided by the Anton Paar software (Version 8.0.20) and was calculated as the slope of friction force over the applied normal force.

Animal Experiments

All the procedures were performed according to the Institutional Animal Care and Use Committee (IACUC) at the National University of Singapore (Protocol number: R17-1410). In all, 11 to 13 months old male micropigs were divided into 4 groups: 1) defect with empty fibrin hydrogel implantation (Control), number of animal (n) = 10; 2) defect with fibrin hydrogel containing autologous TCP expanded FT chondrocytes (TCP FT), n = 10; 3) defect with fibrin hydrogel containing autologous microcarrier expanded FT chondrocytes (dMC FT), n = 12; 4) defect with bilayered fibrin hydrogel (SZ chondrocytes overlaying

MZ/DZ chondrocytes) containing autologous zonal chondrocytes from E/S strategy (dMC Bilayer), n = 12. The timeline of animal experiments is shown in **Figure 1B**. In the first surgery, 8 cartilage plugs (3 mm diameter, 1-2 mm depth) were collected from the NWB region of the trochlea in left knee of each animal with a 3 mm biopsy punch. Collected NWB cartilage plugs were processed to isolate chondrocytes and the isolated chondrocytes were expanded with/without size-based sorting. In the second surgery, critical size bicondylar chondral defects (6 mm diameter, 1 mm depth) were created at the WB regions of the lateral and medial femoral condyles in right knee of each animal with a 6 mm biopsy punch, resulted in 2 defects in each animal. 10 defects were created for Control and TCP FT groups while 12 defects were created for dMC FT and dMC Bilayer groups. Penetration to the subchondral bone was avoided to prevent bleeding. Same implantation was performed on both defects of each animal. In each defect, total volume 50-60 μl fibrin hydrogel with or without cells was delivered. For Group 4, 30 μl of fibrin hydrogel encapsulating MZ/DZ chondrocytes was first delivered to the defect and overlaid with 30 μl of fibrin hydrogel encapsulating SZ chondrocytes. The final fibrinogen, thrombin and cell concentrations were 23 mg/ml, 25 IU and 10 million cells/ml, respectively. All animals were allowed to move freely without immobilization after the surgeries. Animals were euthanised 6 months after the second surgery. The quality of cartilage repair was assessed with a modified O'Driscoll scoring system as shown in **Supplementary Table S2** by 3 blinded and independent researchers.

Magnetic Resonance Imaging (MRI)

The MRI scanning was performed using a 3T whole body MRI scanner (Magnetom Skyra, Siemens; Erlangen, Germany). The following sequences were used: pd_tse_sag_FS_hi-res and pd_tse_cor_FS_hi-res (Voxel size of 0.3 x 0.3 x 2.0 mm; field of view [FOV] read of 140 mm; FOV phase of 100%; slice thickness of 2 mm; repetition time of 2000 ms; time to echo of 13 ms). Syngo fastView software (Siemens Healthineers; Erlangen, Germany) was used in the MRI scan analysis.

Micro-Computed Tomography (microCT)

The micro-CT imaging was performed using microCT scanner (Bruker micro-CT, Kontich, Belgium). About 500 consecutive slices were obtained from each defect with a voxel size of 40 μm/pixel. An X-ray source was adopted to scan at voltage of 90 kV in 20 mm field of view (FOV). CT-Analyzer (Skyscan) was used for the analysis bone resorption volume. VGSTUDIO MAX (Volume Graphics) was used in 3D reconstruction of the micro-CT scan.

Statistical Analysis

The statistical significance between 3 or more groups was evaluated by one-way ANOVA with Tukey post-hoc test. The statistical significance between 2 groups was evaluated by independent-samples t-test. The significance was set at $p<0.05$. All statistical analysis was performed with IBM SPSS statistical software (IBM, USA).

Results

Comparison of NWB and WB Derived Zonal Chondrocyte Phenotypes

The feasibility of size-based separation of zonal chondrocytes from FT NWB chondrocytes using inertial spiral microchannel was evaluated, in comparison to WB chondrocytes. **Supplementary Figure S2** showed increasing cell size from S1 to S3 subpopulations derived from WB and NWB chondrocytes. No significant difference between WB and NWB chondrocytes in respective subpopulations was observed. Similar to WB chondrocytes, NWB S1 was predominantly *PRG4* expressing cells and the expression levels of *ACAN, COL2A1* and *COL9A2* increased with cell size (**Fig. 2A**). The results indicated that NWB FT chondrocytes can be separated into enriched SZ, MZ and DZ chondrocytes, as S1, S2 and S3 subpopulation, respectively, based on cell size using inertial spiral microchannel device. This is similar to the results reported in our previous studies.[17,28]

We then compared the efficacy of post-expansion sorting strategy in producing zonal chondrocytes from WB and NWB FT chondrocytes. The strategy involved the expansion of freshly isolated FT chondrocytes first on TCP for one passage (P1, 2 weeks), then on dMC for 2 passages (P2 and P3, 8 days in each passage), followed by zonal chondrocyte size-based separation. The expand-sort cells, as S1 and S2S3 combine, then underwent 3 weeks of tissue formation in 3D hydrogel, as illustrated in **Figure 1A**.

Histological analysis of the tissue constructs showed that zonal cartilage characteristics was observed in both WB and NWB tissue constructs where Saf-O and Col2 were stained stronger in S2S3 compared to S1 tissue constructs (**Fig. 2B**). Significantly higher percentage of Col9 positive stained cells was observed in S2S3 WB and NWB than their respective S1 constructs ($P < 0.001$; **Fig. 2C**). In contrast, S1 WB and NWB had significantly higher percentage of PRG4 positive stained cells than the respective S2S3 constructs ($P < 0.001$). S2S3 chondrocytes from both WB and NWB regions generated tissue constructs with comparable Youngs' Modulus ($P = 0.99$), with significantly higher strength than their respective S1 constructs ($P = 0.001$ and 0.045 for WB and NWB, respectively; **Fig. 2D**). On the other hand, S1 chondrocytes generated tissue constructs with lower average coefficient of friction as compared to their respective S2S3 constructs, albeit with no significant difference ($P = 0.11$; **Fig. 2D**). The

results indicated that post-expansion sorting strategy can be applied on NWB FT chondrocytes to produce high quality zonal chondrocytes that were able to form cartilage tissues with distinct biochemical and biomechanical zonal properties.

In Vivo Study: Zonal Phenotype of Regenerated Tissues

In healthy articular cartilage, chondrocytes in the deeper zone form an array of 4 to 5 cells in a columnar organization that aligns perpendicularly to the surface. The columnar arrangement of chondrocytes at DZ was maintained in the native tissue adjacent to the regenerated tissues in all study groups (**Fig. 3A**). 2 out of 6 defects in the Control and TCP FT groups, and 3 out of 6 defects in both the dMC groups had their chondrocyte columnar architecture preserved at the edge of regenerated tissues (**Table 1**). The number of samples with columnar organization preserved at the center of the regenerated tissues maintained in Control (2 out of 6 defects) and dMC Bilayer (3 out of 6 defects). However, such columnar arrangement was only observed in 1 out of 6 defects in TCP FT and dMC FT groups. Quantification of DZ chondrocytes columnar arrangement at the center of defects (**Fig. 3B**) showed that the dMC Bilayer has the highest average percentage of DZ chondrocytes in columnar organization, as compared to Control, TCP and dMC FT, although the difference did not reach significance ($P = 0.225$).

PRG4 immuno-staining (**Fig. 4**) showed that PRG4 was localized as a thin layer specifically at the SZ in the healthy articular cartilage tissue. PRG4 was found at the upper region of regenerated tissues in all study group. However dispersed PRG4 distribution was detected in 4 out of 6 defects in Control and 3 out of 6 defects in TCP FT and dMC FT and 2 out of 6 defects in dMC Bilayer groups at the edge of the regenerated tissues (**Table 2**). This dispersed distribution of PRG4 increased further at the center of the regenerated tissues. The dMC Bilayer groups had the highest number of regenerated tissues (4 out of 6 defects) with the closest resemblance of thin PRG4 layer similar to the healthy articular cartilage tissue, at both the edge and center of the regenerated tissues (**Table 1**).

Zonal orientation of collagen fibers in a healthy articular cartilage was demonstrated by polarized light microscopy where distinct optical birefringence of collagen fibers was visible between SZ and MZ/DZ, with a bright thin layer at the SZ and dark scale at the deeper zone (**Fig. 5**). The dMC Bilayer group had the highest number of regenerated tissues showing these distinct zonal differences (4 out of 6 defects) among all the study groups (**Table 1**). These birefringence differences were lacking in the Control group where the collagen fibers were arranged randomly throughout the FT of the regenerated tissues. Only 1 out of 6 defects in TCP FT and 2 out of 6 defects in dMC FT groups had distinct collagen fibers orientation between SZ and deeper zones.
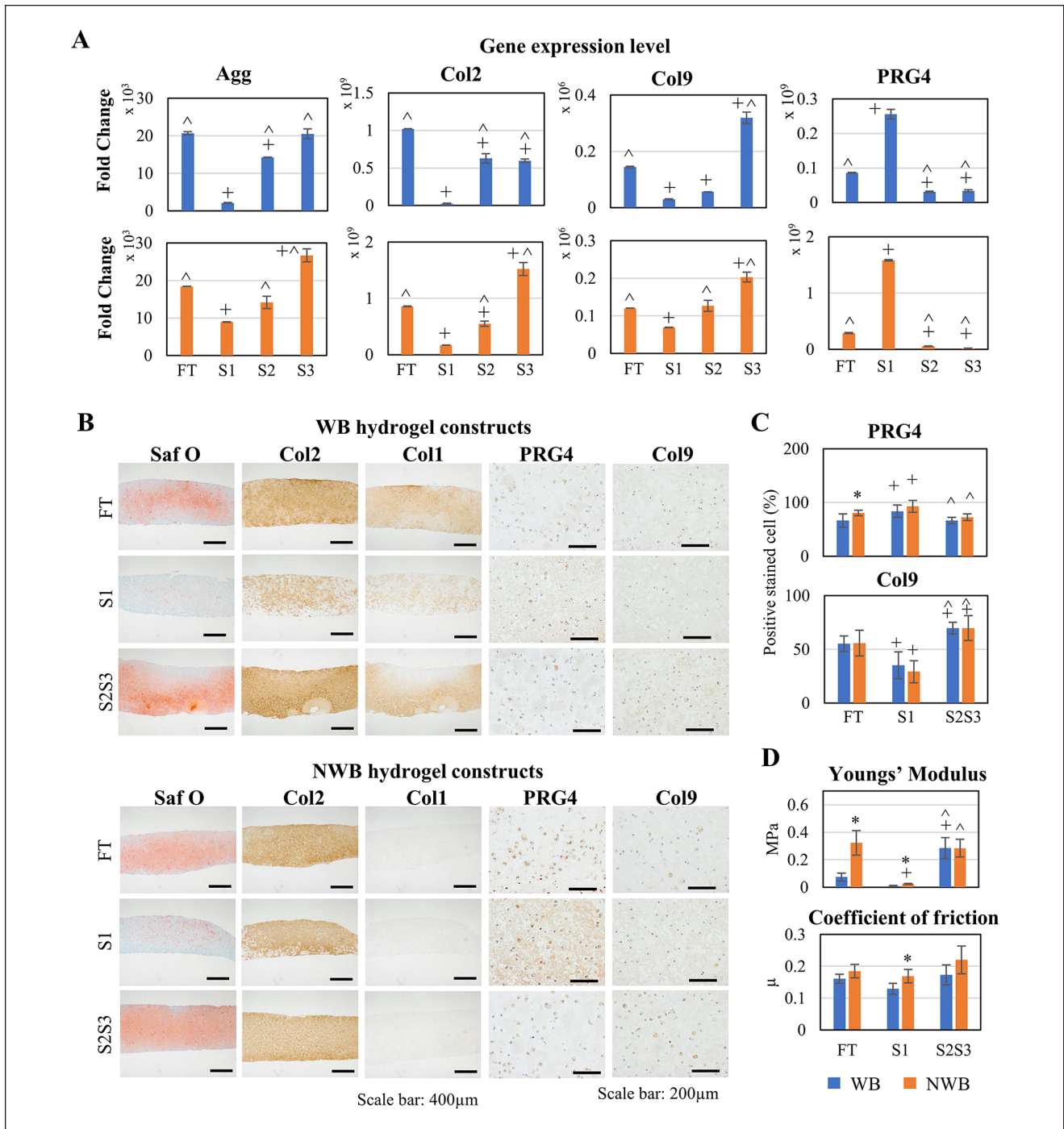
Figure 2. Zonal phenotype characterization of WB and NWB chondrocytes. (**A**) Aggrecan (*ACAN*), Col2 (*COL2A1*), Col9 (*COL9A2*) and PRG4 (*PRG4*) mRNA expression profile of non-expanded FT, size-based sorted small (S1), medium (S2) and large (S3) chondrocytes derived from WB and NWB cartilage. (**B**) Formation of sGAG, Col2, Col1, Col9 and PGR4 in 3D hydrogel, indicated by Saf O staining, and Col2, Col1, Col9 and PRG4 immuno-staining of cartilage constructs. Cartilage constructs were generated from 3-week culture of zonal chondrocytes derived from post-expansion sorting strategy. 40x magnification for Saf O, Col2 and Col staining. 200x magnification for Col9 and PRG4 staining. (**C**) Quantification of PRG4 or Col9 positive cells. (**D**) Mechanical properties of cartilage constructs generated by dMC-expanded FT, S1 and S2S3 chondrocytes isolated from WB and NWB regions, presented as Youngs' modulus and coefficient of friction. Images and results are representative data from 3 independent experiments using chondrocytes extracted from 3 pigs, with triplicate in each experiment. Data is presented as mean ± standard deviation. WB = weight bearing; NWB = non-weight-bearing; FT = full thickness; dMC = dynamic microcarrier. + denotes significant difference compared to FT, and ^ denotes significant difference compared to S1. * denotes significant difference between WB and NWB in corresponding subpopulations.
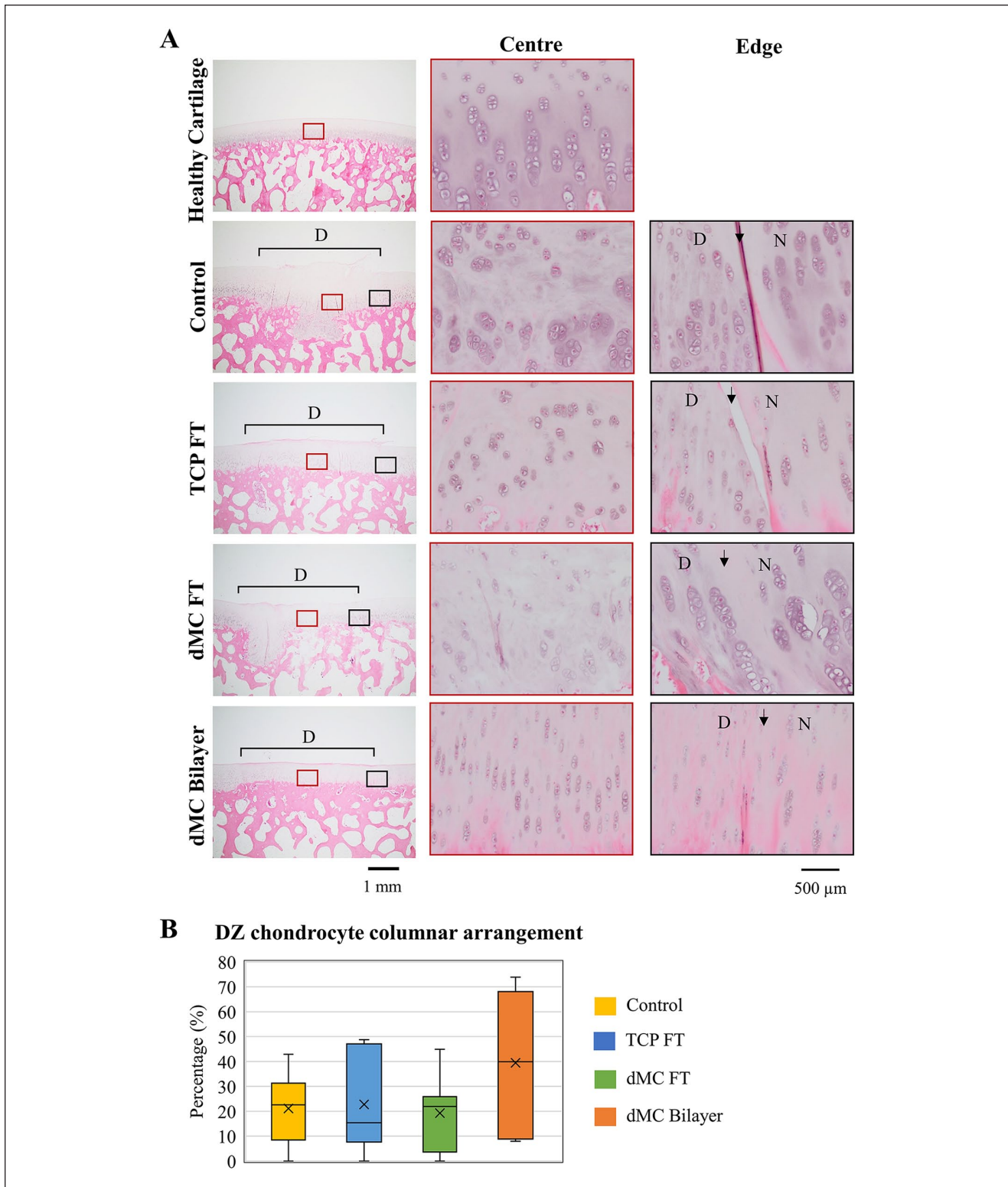
Figure 3. Zonal properties of regenerated tissues. (**A**) H&E staining of the regenerated tissues. 20x magnification for images on first column. 200x magnification for images on second and third column. Images are representative of samples from $n = 6$. (**B**) Quantification of the DZ chondrocyte columnar arrangement. Data is presented as box-and-whiskers plots. The whiskers show the maximum and minimum values; the boxes show the interquartile range; the horizontal lines in the boxes show the median and the X in the boxes show the mean value. $n = 6$ per group. DZ = deep zone; TCP = tissue plate culture platform; FT = full thickness; dMC = dynamic microcarrier.

Table 1. Summary on the Observation on Zonal Characteristic of Regenerated Tissues Based on H&E Staining, PRG4 Immunohistology and Polarized Light Microscopy.

	Control	TCP FT	dMC FT	dMC Bilayer
Columnar chondrocyte organization (H&E staining)				
Edge of defects	2/6 (33.3%)	2/6 (33.3%)	3/6 (50.0%)	3/6 (50.0%)
Center of defects	2/6 (33.3%)	1/6 (16.7%)	1/6 (16.7%)	3/6 (50.0%)
PRG4 localization at SZ (Immunostaining)	2/6 (33.3%)	3/6 (50.0%)	3/6 (50.0%)	4/6 (66.7%)
Distinct collagen alignment at SZ and MZ/DZ (Polarized light microscopy)	0/6 (0%)	1/6 (16.7%)	2/6 (33.3%)	4/6 (66.7%)
Fibrillation (H&E staining)	4/6 (66.7%)	4/6 (66.7%)	3/6 (50.0%)	2/6 (33.3%)

TCP = tissue plate culture platform; FT = full thickness; dMC = dynamic microcarrier; SZ = superficial zone; MZ = middle zone; DZ = deep zone.

In Vivo *Study: Cartilage Characteristics of Regenerated Tissues in Porcine Chondral Defect Model*

Figure 6A showed the representative MRI images of each group. In all, 50% of defects in Control (2 out of 4 defects) and dMC FT (3 out of 6 defects) groups have neo tissues that were thicker than the adjacent native cartilage tissues, over-reaching into the subchondral bone region, indicative of subchondral bone defects (**Supplementary Fig. S3** and **Table 2**). On the other hand, neo tissues in 50% of the defects in TCP FT group (2 out of 4) were thinner than adjacent native cartilage tissues, suggesting of subchondral bone plate advancement into the cartilage layer. By contrast, only 1 defect in the dMC Bilayer group had cartilage penetrating the subchondral bone and 1 defect had relatively thin regenerated tissue than the adjacent native tissues, out of the 6 defects. The rest of the regenerated tissues (66.7%) of the dMC Bilayer group showed regenerated cartilage layer with similar thickness to the surrounding native cartilage tissues.

Representative microCT sections at the center of defects in each group were demonstrated in **Figure 6B**. The results showed that the dMC Bilayer had the lowest number of subchondral bone defect cases (1 out of 6 defects), compared to dMC FT (4 out of 6 defects), TCP FT (2 out of 6 defects) and the Control (5 out of 6 defects) groups (**Supplementary Fig. S4 and Table 2**). On the other hand, bone overgrowth was most common in TCP FT group where it happened in 50% of the total number of defects while the percentage decreased to 33.3%, 16.7 and 16.7% in Control, dMC FT and dMC Bilayer groups, respectively. The subchondral bone health was further assessed with subchondral bone uniformity scoring where dMC Bilayer group had significantly higher score at than Control and dMC FT group ($P = 0.005$ and 0.028 for Control and dMC FT, respectively) (**Table 2**). In contrast, no significant difference was registered between dMC FT group and Control ($P = 0.58$) or TCP FT group ($P = 0.97$).

Differences could be observed between groups in terms of sulphated glycosaminoglycans (sGAG) contents. The Saf O staining for 4 out of 6 defects (66.7%) in Control group, 5 out of the 6 defects (83.3%) in each of the TCP FT and dMC FT group, and 3 out of 6 defects (50%) in dMC Bilayer group were unsatisfactory when compared to heathy cartilage tissue (**Supplementary Fig. S5**). Control and TCP FT each had 2 defects lightly stained for Saf O while dMC FT had 1 defect lightly stained for Saf O. Furthermore, 4 defects in dMC FT, 3 defects in each of the TCP and dMC Bilayer groups and 2 defects in the Control were devoid of sGAG at SZ and a partial region of MZ in the regenerated tissues. Negative Saf O staining was consistent in the protrusion or fibrillation surface of regenerated tissue, similar to the observation reported by other groups.[32] Subchondral bone defect was also apparent in tissue sections of 4 out of 6 (66.7%) defects in Control and dMC FT groups, and 2 out of 6 (33.3%) defects in TCP FT and dMC Bilayer group. The variability in the quality of the regenerated tissues within each treatment group resulted in no significant difference across the groups ($P = 0.80$) in the Histology Score (**Supplementary Fig. S6A**). However, the differences in surface smoothness of the regenerated tissues following different treatment methods can be observed in H&E staining (**Supplementary Fig. S7** and **Table 1**) where the fibrillation was evident in 4 out of 6 defects in Control and TCP FT groups, 3 out of 6 defects in dMC FT group and 2 out of 6 defects dMC Bilayer groups. The functionally of regenerated tissues indicated by compression test demonstrated that the implantation of dynamic microcarrier expanded chondrocytes yielded regenerated tissues with significantly enhanced Youngs' Modulus in dMC FT and dMC Bilayer groups, compared to TCP FT group ($P = 0.03$) (**Supplementary Fig. S6B**). In contrast, TCP FT chondrocytes implantation did not improve the Youngs' Modulus, relative to Control hydrogel implantation.

Discussion

The beneficial effect of zonal chondrocyte bilayered implantation for articular cartilage regeneration has previously been demonstrated using freshly isolated chondrocytes or
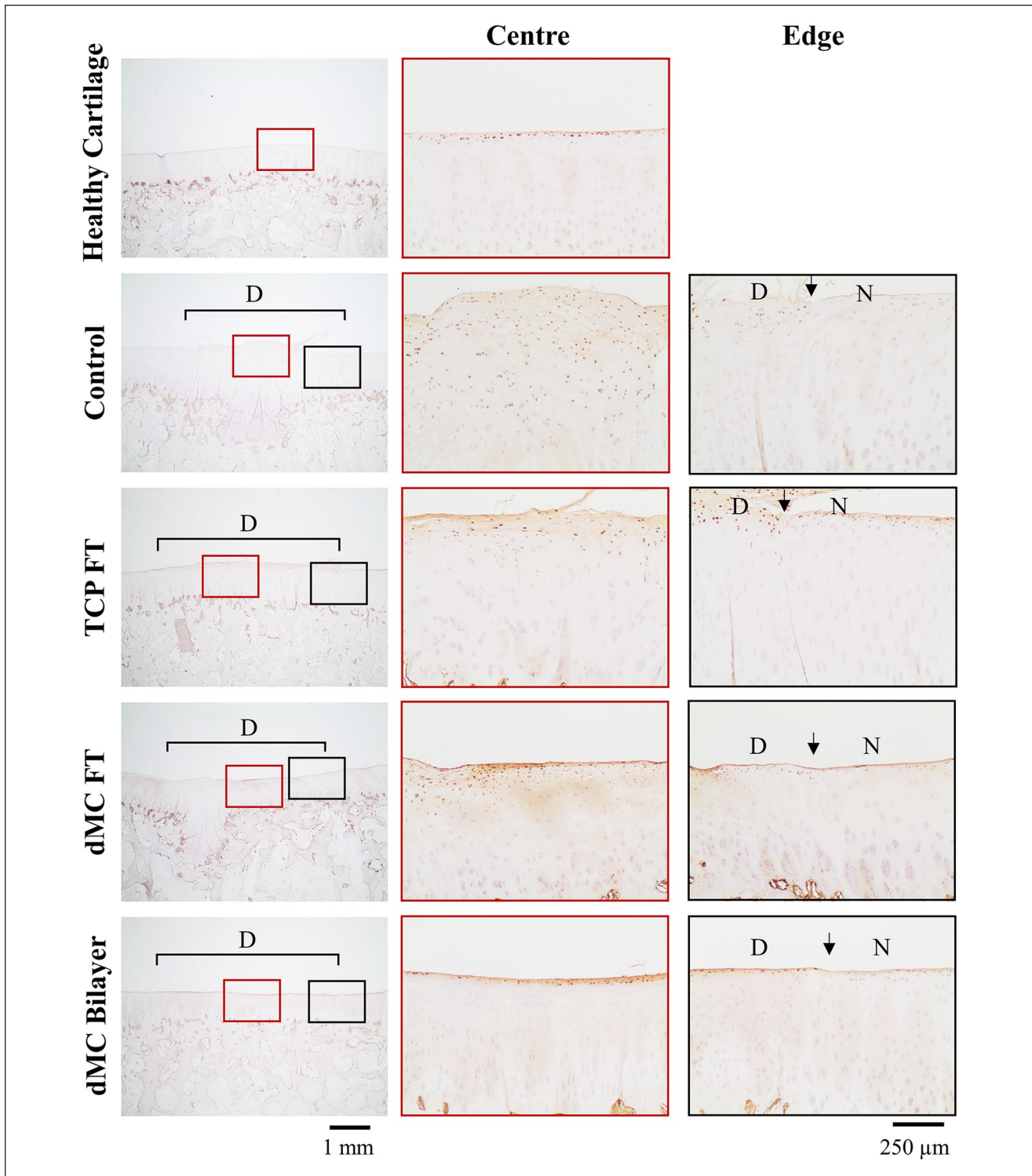
Figure 4. Zonal properties of regenerated tissues. Immunohistochemical analysis of SZ specific protein, PRG4, by immuno-staining. 20x magnification for images on first column. 100x magnification for images on second and third column. Center indicates center of the defects labeled by red boxes; Edge indicates the right edge of defects labeled by black boxes. SZ = superficial zone; N = native tissues; D = defects; TCP = tissue plate culture platform; FT = full thickness; dMC = dynamic microcarrier. Arrows indicate the sites of the defect edge. Images are representative of samples from $n = 6$ per group.

Table 2. Summary on the Observation on Structural Integrity of Subchondral Bone Based on MRI Analysis and MicroCT Imaging.

	Control	TCP FT	dMC FT	dMC Bilayer
MRI				
Subchondral bone defects	2/4 (50%)	0/4 (0%)	3/6 (50.0%)	1/6 (16.7%)
Articular cartilage thinning	0/4 (0%)	2/4 (50%)	0/6 (0%)	1/6 (16.7%)
MicroCT				
Subchondral bone defects	5/6 (83.3%)	2/6 (33.3%)	4/6 (66.7%)	1/6 (16.7%)
Subchondral bone overgrowth	2/6 (33.3%)	3/6 (50.0%)	1/6 (16.7%)	1/6 (16.7%)
Subchondral bone uniformity scoring	1.83 ± 0.41	2.17 ± 0.41	2.08 ± 0.29	2.67 ± 0.52[a,b]

Subchondral bone uniformity scoring are presented as mean ± standard deviation, *n* = 6 per group. Subchondral bone with uniform surface = 3;
Subchondral bone with erosion or advancement = 2; Subchondral bone with both erosion and advancement = 1.
MRI = Magnetic Resonance Imaging; TCP = tissue plate culture platform; FT = full thickness; dMC = dynamic microcarrier.
[a]denotes significant difference as compared to control.
[b]denotes significant difference as compared to dMC FT.
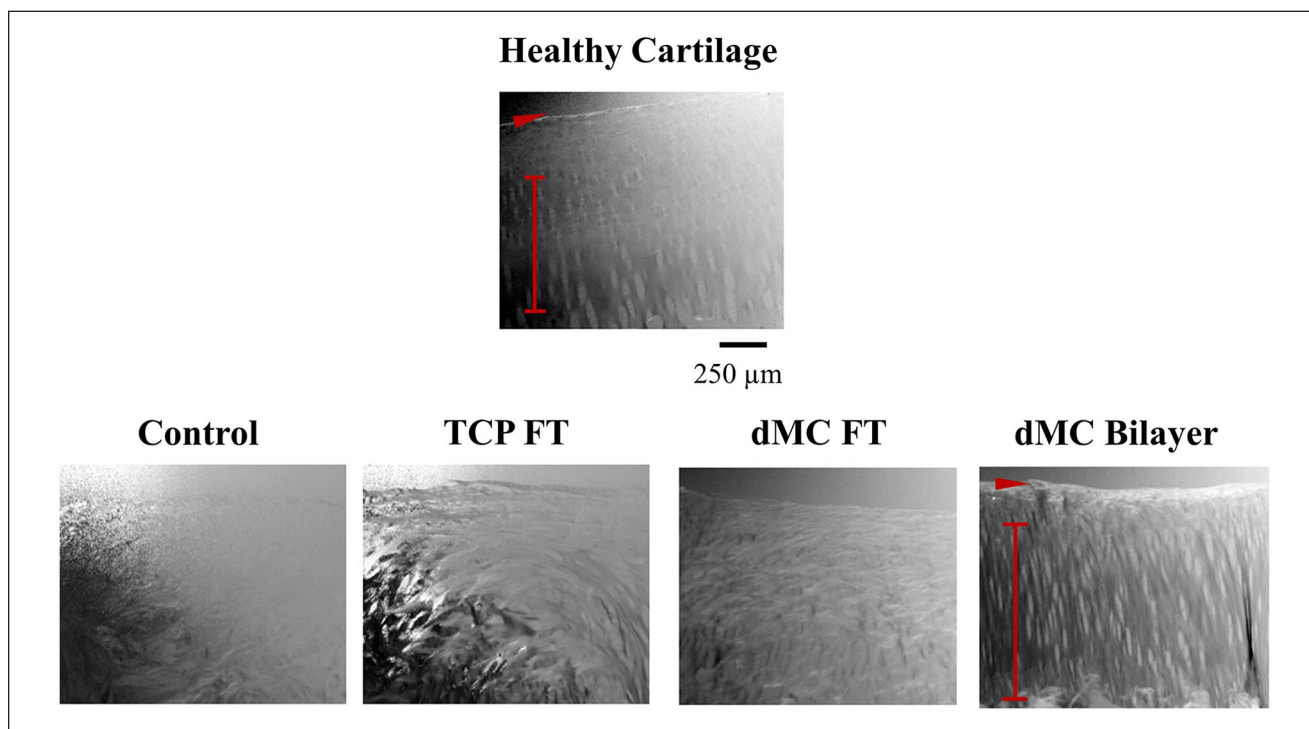

Figure 5. Polarized light microscopy images of healthy articular cartilage tissues and regenerated tissues taken at the center of defects. The collagen fibers arranged parallel to the articular surface are indicated by red arrowhead and the collagen fibers arranged perpendicular to the articular surface are indicated by red line. 100x magnification. Images are representative of samples from n = 6 per group. TCP = tissue plate culture platform; FT = full thickness; dMC = dynamic microcarrier.

pre-differentiated MSC-derived chondrocytes on rodent and rabbit osteochondral defect models.[17,33] The proof-of-concept studies were however followed up over a short-term recovery period of up to 6 or 12 weeks. Moreover, the cartilage defect sites in both the rat and rabbit models were at the non-weight bearing region of the trochlea. In this study, the regenerative efficacy of zonal chondrocyte bilayered implantation was validated using a porcine model that has anatomically similar knee joints as humans, with cartilage defects created at the femoral condyles that was subjected to similar mechanical microenvironment akin to the weightbearing portion of the human cartilage lesion. In addition, having previously shown the regenerative efficacy of freshly isolated zonal chondrocytes,[17] this study progressed to demonstrate the effectiveness of culture expanded zonal chondrocytes generated using our established dMC post-expansion sorting strategy as illustrated in **Figure 1A**.[28] Further, to mimic the current ACI surgery procedure,[29] the
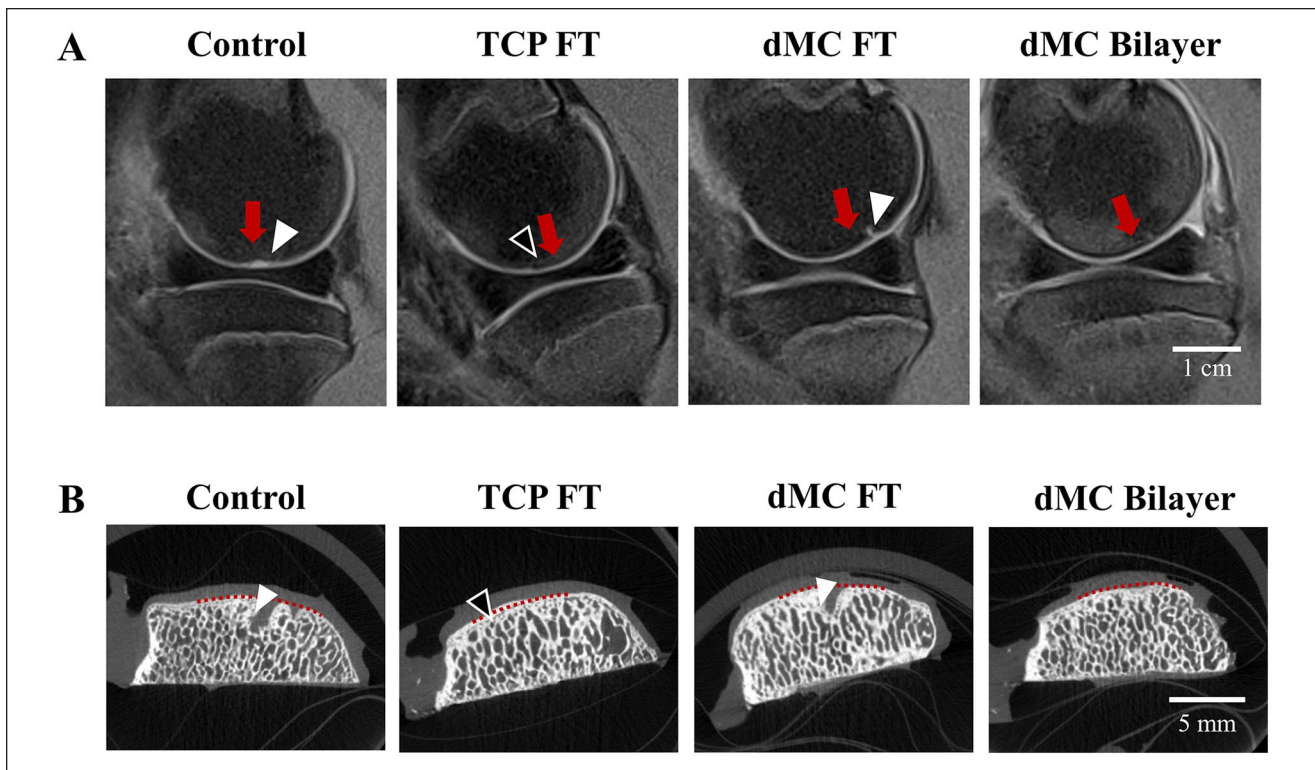
Figure 6. (**A**) MRI images of the knees harvested from Control, TCP FT, dMC FT or dMC Bilayer groups. Red arrow indicates the location of defects; white arrowhead indicates the subchondral bone erosion; black arrowhead indicates the cartilage thinning. The scale bar in the dMC Bilayer group applied to all images in the Figure. (**B**) The cross-section of microCT scan at the center of defects. Red dashed line indicates the imaginary boundary of the healthy subchondral bone surface. The scale bar in the dMC Bilayer group applied to all images in the Figure. Images are representative data from 4-6 samples per group. MRI = Magnetic Resonance Imaging; TCP = tissue plate culture platform; FT = full thickness; dMC = dynamic microcarrier.

implanted cells was derived from the autologous osteochondral plug excised from the NWB trochlea of the animals as shown in **Figure 1B**.

We first demonstrated that chondrocytes derived from NWB cartilage tissue can be sorted by size using the spiral microchannel device into zonal chondrocyte subpopulations (**Fig. 2A**). dMC post-expansion sorting strategy was equally effective in generating large quantities of expanded zonal chondrocytes from both WB and NWB cartilage tissues that are capable in generating cartilage tissues construct with distinct biochemical and biomechanical zonal properties (**Fig. 2B-D**). On average, $0.83 \pm 0.45 \times 10^6$ of chondrocytes can be isolated from NWB articular cartilage plugs in minipig, with minimum number at $\sim 0.17 \times 10^6$. This is similar to the number of autologous chondrocytes that can be isolated from a patient in the clinical setting that ranges from 0.18 to 0.455×10^6 chondrocytes.[29] With the post-expansion sorting strategy, the projected cell yields for SZ and MZ/DZ chondrocytes were 1.3 and 5.1×10^6, respectively, from a starting cell number of 0.17×10^6. Based on the implantation cell density of 10×10^6 cells per milli-liter, the number of chondrocytes produced by our

expansion/sort strategy is hence sufficient to treat articular cartilage defects of at least 5 cm^2, which falls within the range of lesion mean size (4.8 to 8.4 cm^2) reported by various clinical studies.[34-36]

The regenerative efficacy of dMC expanded and spiral microchannel sorted NWB zonal chondrocytes delivered as bilayered zonal chondrocyte implantation in a porcine chondral defect model was compared to TCP-expanded FT chondrocytes (TCP FT, the current ACI cell source) and dMC expanded FT chondrocytes, to provide unequivocal validation to the benefit of the bilayered implantation approach (**Fig. 1B**). Although the regenerated tissues in dMC FT and dMC Bilayer group have similar histology (**Supplementary Fig. S6A**) and mechanical strength (**Supplementary Fig. S6B**), the dMC Bilayer group generated tissues with better zonal organization [**Figs. 3-5** and **Table 1**). Consistently higher cases have formation of columnar chondrocytes in the DZ (**Fig. 3**), specific localization of PRG4 in SZ (**Fig. 4**), and development of stratified cartilage tissue apparent under polarized light microscopy (**Fig. 5**), that was more akin to normal cartilage tissue. The observation of PRG4-positive chondrocytes

concentrated at the upper region of regenerated tissues in the Control, TCP FT and dMC FT group was possibly developed as a consequence of in situ mechanical-induced zonal characteristic conversion, given the known plasticity of chondrocytes[16,37-39] (**Fig. 4**). However, majority of the PRG4-positive chondrocytes in these groups have dispersed distribution instead of the tight SZ layer in the normal articular cartilage. It was demonstrated previously that distinct layers of zonal chondrocytes can be preserved for at least 2 to 4 weeks post implantation at the defect site when delivered as bilayered fibrin constructs.[17,33] It is thus likely that the positioning of the defined layers of SZ over M/DZ chondrocytes in the dMC Bilayer group has contributed to the immediate *in situ* surface lubrication of the implanted constructs, while established the compressive strength in the deeper zones, possibly facilitated the shear-compression induced development of zonal characteristic and collagen fibril organization across the cartilage zones.[40,41] Implantation of stratified cartilaginous constructs with expanded superficial and middle chondrocyte subpopulations was previously attempted in mini-pigs using a scaffold free system.[23,24] The zonal architecture maintained for 4 weeks *in vitro* was lost 1-week post-implantation. This could be due to the weak matrix content of the implanted constructs that were not able to maintain the zonal chondrocytes in their respective location when exposed to the harsh mechanical environment *in vivo*. Our approach of using fibrin hydrogel delivered as bilayered constructs encapsulating zonal chondrocytes helped to retain the zonal chondrocytes in their respective positions. Furthermore, zonal chondrocytes derived from dMC were less de-differentiated and likely formed cartilage matrix more efficiently as compared to monolayer expanded and de-differentiated chondrocytes.

The perpendicular arrangement of collagen fibers that were directed against the compressive force served as a damping system to resist lateral fluid flow during compression[7,8] and anchored the regenerated cartilage to the underlying subchondral bone.[3,9] This would enable the articular cartilage to resist loading force without significant deformation of its solid matrix[8] in the dMC Bilayer group, while the organized SZ collagen fibers would reduce the articular cartilage permeability and enhance the fluid load support to the underlying zone.[4,5] On the other hand, the lack of organized 3D structural properties in the regenerated tissues could lead to susceptibility to physical and physiological stresses.[42] Accordingly, a higher prevalence of subchondral bone abnormalities was detected in the Control, TCP FT and dMC FT groups relative to the dMC Bilayer group [**Fig. 6, Table 2** and **Supplementary Figs. S3 and S4**]. Notably, the subchondral bone scoring of dMC Bilayer group was significantly higher, while similar lower scorings were registered with dMC FT and TCP FT or Control groups (**Table 2**).

The cartilage-bone interface served to maintain structural integrity of the subchondral bone during articular joint motion.[9] During the creation of critical size chondral defects, disruption to the cartilage-bone interface was inevitable, hence would have subjected the subchondral bone at the defect sites to remodeling. Different paracrine activities of SZ and DZ chondrocytes could have influence the homeostasis of the subchondral bone. DZ chondrocytes has been reported to support mineralization, while SZ chondrocytes, through the action of PTHrP secretion, suppressed mineralization.[43] The positioning of DZ chondrocytes next to the subchondral bone in the dMC Bilayer implantation could have facilitate the restoration of the disrupted cartilage-bone interface induced during surgery. On the other hand, dMC-FT implantation in which proximity of SZ near the subchondral bone in the mixed chondrocyte population might cause inhibition to mineralization, further compounded to bone erosion. It is known that the changes in subchondral bone can affect the long-term survival of the regenerated tissues.[44,45] Hence, despite the similar performance between dMC FT and dMC Bilayer in terms of histology scoring and mechanical properties at the 6-month time point of tissue analysis, defect site tissues in dMC Bilayer group could be superior in providing long-term integrity of the regenerated tissue than dMC FT with their capability in recapitulating the zonal characteristic of native articular cartilage tissues and maintaining integral subchondral bone.

Even though a general trend of improvement in bilayered implantation of zonal chondrocytes was observed, the high variability of the treatment outcomes offset the statistical significance between groups (**Supplementary Fig. S6**). The use of autologous chondrocytes and the large variation in animal weight could have contributed to the discrepancy. Although the animals were at about the same age ($\pm$ 2 months old), their weight range from 13.3 to 25.9 kg. This would have exposed the implanted chondrocytes to different levels of mechanical stress. Furthermore, the bicondylar defect model used in this study could have increased the burden and instability of the knee joints, resulting in the variable distribution of mechanical stress to the lateral and medial femoral condyle defects in each animal. Lastly, the weight bearing region of articular cartilage could compromised the integrity of the fibrin hydrogel. A biomaterial with more compatible mechanical properties could further improve the repair outcomes. The integrity of the regenerated tissues from bilayered zonal chondrocyte implantation should be further verified with a longer-term animal experiment that last for at least a year with a better control on the variables such as the animal size, the use of single condylar defects and a more appropriate delivery carrier. Nevertheless, the results from this medium-term *in vivo* study suggest the benefit of bilayered implantation of zonal chondrocytes in improving cartilage regeneration at

the levels of biochemical and mechanical strength, and in particular, the zonal architecture of the regenerated cartilage tissues and subchondral bone integrity. Further animal study would be warranted to decipher the events of bone remodeling at the bone cartilage-interface at the early stage of repair, as well as evaluate the integrity of the regenerated tissue after longer term of recovery period.

Conclusion

Current ACI strategies employ a heterogeneous mixture of expanded chondrocytes. The zonal repair of cartilage lesions with stratified implantation of zonal chondrocytes have yet to be realized due to the inefficient zonal chondrocyte isolation process, limited availability of autologous chondrocytes and chondrocyte dedifferentiation after expansion. In this study, we showed that the dynamic microcarrier culture expanded and size-based sorted zonal chondrocytes can overcome the clinical challenges to produce sufficient number of zonal chondrocytes from the limited amount of clinically relevant NWB cartilage plugs to support autologous stratified zonal chondrocyte implantation. This 6-month pre-clinical porcine cartilage repair study showed improved regenerative efficacy of bilayered zonal chondrocyte implantation that encouraged the regeneration of zonal architecture and healthier underlying subchondral bone. Taken together, with appropriate expansion of zonal chondrocytes, the strategy of stratified zonal chondrocyte implantation could represent a significant advancement to current ACI-based cartilage regeneration, with the potential to improve the long-term integrity of the regenerated cartilage tissues.

Declaration of Conflicting Interests

The author(s) declared no potential conflicts of interest with respect to the research, authorship, and/or publication of this article.

Ethical Approval

All the procedures in animal experiments were performed according to the Institutional Animal Care and Use Committee (IACUC) at the National University of Singapore (Protocol number: R17-1410).

ORCID iD

Ching Ann Tee   https://orcid.org/0000-0002-1186-8580

References

1. Klein TJ, Malda J, Sah RL, Hutmacher DW. Tissue engineering of articular cartilage with biomimetic zones. Tissue Eng Part B Rev. 2009;15(2):143-57.

2. Hayes AJ, Hall A, Brown L, Tubo R, Caterson B. Macromolecular organization and in vitro growth characteristics of scaffold-free neocartilage grafts. J Histochem Cytochem. 2007;55(8):853-66.

3. Sophia Fox AJ, Bedi A, Rodeo SA. The basic science of articular cartilage: structure, composition, and function. Sports Health. 2009;1(6):461-8.

4. Gannon AR, Nagel T, Kelly DJ. The role of the superficial region in determining the dynamic properties of articular cartilage. Osteoarthr Cartil. 2012;20(11):1417-25.

5. Gannon AR, Nagel T, Bell AP, Avery NC, Kelly DJ. The changing role of the superficial region in determining the dynamic compressive properties of articular cartilage during postnatal development. Osteoarthritis Cartilage. 2015;23(6):975-84.

6. Jay GD, Waller KA. The biology of lubricin: near frictionless joint motion. Matrix Biol. 2014;39:17-24.

7. Hughes LC, Archer CW, Ap Gwynn I. The ultrastructure of mouse articular cartilage: collagen orientation and implications for tissue functionality. A polarised light and scanning electron microscope study and review. Eur Cell Mater. 2005;9(68):e84.

8. Ap Gwynn I, Wade S, Ito K, Richards RG. Novel aspects to the structure of rabbit articular cartilage. Eur Cell Mater. 2002;4(Suppl 1):18-29.

9. Hoemann CD, Lafantaisie-Favreau C-H, Lascau-Coman V, Chen G, Guzmán-Morales J. The cartilage-bone interface. J Knee Surg. 2012;25(2):85-98.

10. Blumbach K, Bastiaansen-Jenniskens YM, DeGroot J, Paulsson M, van Osch GJ, Zaucke F. Combined role of type IX collagen and cartilage oligomeric matrix protein in cartilage matrix assembly: cartilage oligomeric matrix protein counteracts type IX collagen-induced limitation of cartilage collagen fibril growth in mouse chondrocyte cultures. Arthritis Rheum. 2009;60(12):3676-85.

11. Haleem-Smith H, Calderon R, Song Y, Tuan RS, Chen FH. Cartilage oligomeric matrix protein enhances matrix assembly during chondrogenesis of human mesenchymal stem cells. J Cell Biochem. 2012;113(4):1245-52.

12. Knutsen G, Engebretsen L, Ludvigsen TC, Drogset JO, Grøntvedt T, Solheim E, et al. Autologous chondrocyte implantation compared with microfracture in the knee: a randomized trial. J Bone Joint Surg Am. 2004;86(3):455-64.

13. Blewis ME, Schumacher BL, Klein TJ, Schmidt TA, Voegtline MS, Sah RL. Microenvironment regulation of PRG4 phenotype of chondrocytes. J Orthop Res. 2007;25(5):685-95.

14. Ng KW, Ateshian GA, Hung CT. Zonal chondrocytes seeded in a layered agarose hydrogel create engineered cartilage with depth-dependent cellular and mechanical inhomogeneity. Tissue Eng Part A. 2009;15(9):2315-24.

15. Sharma B, Williams CG, Kim TK, Sun D, Malik A, Khan M, et al. Designing zonal organization into tissue-engineered cartilage. Tissue Eng. 2007;13(2):405-14.

16. Schuurman W, Klein TJ, Dhert WJA, Van Weeren PR, Hutmacher DW, Malda J. Cartilage regeneration using zonal chondrocyte subpopulations: a promising approach or an overcomplicated strategy? J Tissue Eng Regen Med. 2015;9(6):669-78.

17. Yin L, Wu Y, Yang Z, Denslin V, Ren X, Tee CA, *et al*. Characterization and application of size-sorted zonal chondrocytes for articular cartilage regeneration. Biomaterials. 2018;165:66-78.

18. Woodfield TB, Van Blitterswijk CA, De Wijn J, Sims TJ, Hollander AP, Riesle J. Polymer scaffolds fabricated with pore-size gradients as a model for studying the zonal organization within tissue-engineered cartilage constructs. Tissue Eng. 2005;11(9-10):1297-311.

19. Owida HA, Yang R, Cen L, Kuiper NJ, Yang Y. Induction of zonal-specific cellular morphology and matrix synthesis for biomimetic cartilage regeneration using hybrid scaffolds. J R Soc Interface. 2018;15(143):20180310.

20. Camarero-Espinosa S, Rothen-Rutishauser B, Weder C, Foster EJ. Directed cell growth in multi-zonal scaffolds for cartilage tissue engineering. Biomaterials. 2016;74:42-52.

21. Dimaraki A, Díaz-Payno PJ, Minneboo M, Nouri-Goushki M, Hosseini M, Kops N, *et al*. Bioprinting of a zonal-specific cell density scaffold: a biomimetic approach for cartilage tissue engineering. Appl Sci. 2021;11(17):7821.

22. Klein TJ, Schumacher BL, Schmidt TA, Li KW, Voegtline MS, Masuda K, *et al*. Tissue engineering of stratified articular cartilage from chondrocyte subpopulations. Osteoarthr Cartil. 2003;11(8):595-602.

23. Chawla K, Klein TJ, Schumacher BL, Jadin KD, Shah BH, Nakagawa K, *et al*. Short-term retention of labeled chondrocyte subpopulations in stratified tissue-engineered cartilaginous constructs implanted in vivo in mini-pigs. Tissue Eng. 2007;13(7):1525-37.

24. Chawla K, Klein TJ, Schumacher BL, Jadin KD, Schmidt TA, Nakagawa K, *et al*. Tracking donor chondrocytes in stratified tissue-engineered cartilage after implantation in vivo. Trans Orthop Res Soc. 2004;29:306.

25. Ng KW, Wang CC, Mauck RL, Kelly TN, Chahine NO, Costa KD, *et al*. A layered agarose approach to fabricate depth-dependent inhomogeneity in chondrocyte-seeded constructs. J Orthop Res. 2005;23(1):134-41.

26. Sharma B, Williams CG, Kim TK, Malik A, Elisseeff JH. Multi-layered hydrogel constructs recreate zonal organization of articular cartilage. Poster presented at 49th Annual Meeting of the Orthopaedic Research Society; February 2-5, 2003; New Orleans, LA.

27. Schuurman W, Harimulyo EB, Gawlitta D, Woodfield TB, Dhert WJ, van Weeren PR, *et al*. Three-dimensional assembly of tissue-engineered cartilage constructs results in cartilaginous tissue formation without retainment of zonal characteristics. J Tissue Eng Regen Med. 2016;10(4):315-24.

28. Tee CA, Yang Z, Yin L, Wu Y, Han J, Lee EH. Improved zonal chondrocyte production protocol integrating size-based inertial spiral microchannel separation and dynamic microcarrier culture for clinical application. Biomaterials. 2019;220:119409.

29. Brittberg M, Lindahl A, Nilsson A, Ohlsson C, Isaksson O, Peterson L. Treatment of deep cartilage defects in the knee with autologous chondrocyte transplantation. N Engl J Med. 1994;331(14):889-95.

30. McCulloch RS, Ashwell MS, O'Nan AT, Mente PL. Identification of stable normalization genes for quantitative real-time PCR in porcine articular cartilage. J Anim Sci Biotechnol. 2012;3(1):36.

31. Lopa S, Ceriani C, Cecchinato R, Zagra L, Moretti M, Colombini A. Stability of housekeeping genes in human intervertebral disc, endplate and articular cartilage cells in multiple conditions for reliable transcriptional analysis. Eur Cell Mater. 2016;31:395-406.

32. Stoop R, Buma P, van der Kraan PM, Hollander AP, Billinghurst RC, Meijers TH, *et al*. Type II collagen degradation in articular cartilage fibrillation after anterior cruciate ligament transection in rats. Osteoarthritis Cartilage. 2001;9(4):308-15.

33. Wu Y, Yang Z, Denslin V, Ren XF, Lee CS, Yap FL, *et al*. Repair of osteochondral defects with predifferentiated mesenchymal stem cells of distinct phenotypic character derived from a nanotopographic platform. Am J Sports Med. 2020;48:1735-47.

34. Beris AE, Lykissas MG, Kostas-Agnantis I, Manoudis GN. Treatment of full-thickness chondral defects of the knee with autologous chondrocyte implantation: a functional evaluation with long-term follow-up. Am J Sports Med. 2012;40(3):562-7.

35. Minas T, Von Keudell A, Bryant T, Gomoll AH. The John Insall Award: a minimum 10-year outcome study of autologous chondrocyte implantation. Clin Orthop Relat Res. 2014;472(1):41-51.

36. Saris D, Price A, Widuchowski W, Bertrand-Marchand M, Caron J, Drogset JO, *et al*. Matrix-applied characterized autologous cultured chondrocytes versus microfracture: two-year follow-up of a prospective randomized trial. Am J Sports Med. 2014;42(6):1384-94.

37. Vanderploeg EJ, Wilson CG, Levenston ME. Articular chondrocytes derived from distinct tissue zones differentially respond to in vitro oscillatory tensile loading. Osteoarthritis Cartilage. 2008;16(10):1228-36.

38. Mizuno S, Ogawa R. Using changes in hydrostatic and osmotic pressure to manipulate metabolic function in chondrocytes. Am J Physiol Cell Physiol. 2011;300(6):C1234-145.

39. Wong M, Siegrist M, Goodwin K. Cyclic tensile strain and cyclic hydrostatic pressure differentially regulate expression of hypertrophic markers in primary chondrocytes. Bone. 2003;33(4):685-93.

40. Rieppo J, Hyttinen MM, Halmesmaki E, Ruotsalainen H, Vasara A, Kiviranta I, *et al*. Changes in spatial collagen content and collagen network architecture in porcine articular cartilage during growth and maturation. Osteoarthritis Cartilage. 2009;17(4):448-55.

41. Gannon AR, Nagel T, Bell AP, Avery NC, Kelly DJ. Postnatal changes to the mechanical properties of articular cartilage are driven by the evolution of its collagen network. Eur Cell Mater. 2015;29(105):103-21.

42. Caldwell KL, Wang J. Cell-based articular cartilage repair: the link between development and regeneration. Osteoarthritis Cartilage. 2015;23(3):351-62.

43. Jiang J, Leong NL, Mung JC, Hidaka C, Lu HH. Interaction between zonal populations of articular chondrocytes suppresses chondrocyte mineralization and this process is mediated by PTHrP. Osteoarthritis Cartilage. 2008;16(1):70-82.

44. Gomoll AH, Madry H, Knutsen G, van Dijk N, Seil R, Brittberg M, *et al*. The subchondral bone in articular cartilage repair: current problems in the surgical management. Knee Surg Sports Traumatol Arthrosc. 2010;18(4):434-47.

45. Imhof H, Breitenseher M, Kainberger F, Rand T, Trattnig S. Importance of subchondral bone to articular cartilage in health and disease. Top Magn Reson Imaging. 1999;10(3):180-92.